Structural Engineering and Mechanics, Vol. 23, No. 2 (2006) 163-175
DOI: http://dx.doi.org/10.12989/sem.2006.23.2.163

Transient response of a piezoelectric layer with a penny-shaped crack under electromechanical impacts

Wenjie Feng†, Yansong Li‡ and DeLiang Ren‡†

Department of Mechanics and Engineering Science, Shijiazhuang Railway Institute, Shijiazhuang 050043, P. R. China

(Received June 27, 2005, Accepted February 3, 2006)

Abstract. In this paper, the dynamic response of a piezoelectric layer with a penny-shaped crack is investigated. The piezoelectric layer is subjected to an axisymmetrical action of both mechanical and electrical impacts. Two kinds of crack surface conditions, i.e., electrically impermeable and electrically permeable, are adopted. Based upon integral transform technique, the crack boundary value problem is reduced to a system of Fredholm integral equations in the Laplace transform domain. By making use of numerical Laplace inversion the time-dependent dynamic stress and electric displacement intensity factors are obtained, and the dynamic energy release rate is further derived. Numerical results are plotted to show the effects of both the piezoelectric layer thickness and the electrical impact loadings on the dynamic fracture behaviors of the crack tips.

Keywords: piezoelectric layer; penny-shaped crack; dynamic energy release rate; dynamic stress intensity factor; axis symmetry.

1. Introduction

Because of their coupled mechanical and electrical properties, piezoelectric ceramics have recently attracted significant attention for their potential application as sensors for monitoring. For example, they can be used in active vibration and noise suppression of sensors in space structures, rockets, weapon systems, smart skin systems of submarines, and so on. The reliability of these structures depends on the knowledge of applied mechanical and electrical disturbance.

Due to the disadvantage of their brittleness, piezoelectric materials have a tendency to develop critical cracks during the manufacturing and poling process. The existence of these defects will greatly affect the mechanical integrity and electromechanical behaviors of this class of material. Since the pioneering studies of Parton (1976) and Deeg (1980) on fracture mechanics of piezoelectric materials, a considerable number of researching works on the electroelastic behaviors of piezoelectric ceramics with defects have been made in past years, and most of these contributions are concentrated on antiplane problems and plane problems. For general 3D crack problem of

† Professor, Corresponding author, E-mail: fengwj@sjzri.edu.cn
‡ Postgraduate Student
‡† Professor

piezoelectric materials, due to the complexity of the mathematical treatment, only a few achievements were reported (Chen and Shioya 1999, 2000). Comparatively speaking, axisymmetrical penny-shaped crack problem as a special kind of 3D problem, great progress has been made. For example, the field intensity factors of a penny-shaped crack for several different loading cases were respectively given (Kogan *et al.* 1996, Karapetian *et al.* 2000, Chen *et al.* 2000, Yang 2004). Eriksson (2002) obtained the energy release rate (ERR) for a penny-shaped crack in a linear piezoelectric solid. Lin *et al.* (2003) derived the stress intensity factor (SIF), ERR and energy density factor (EDF) for the exact and impermeable crack models under mode I loading. Yang and Lee (2003a, 2003b) analyzed the problem of a penny-shaped crack in a piezoelectric cylinder and in a piezoelectric cylinder surrounded by an elastic medium, respectively. Wang *et al.* (2001) studied and numerically calculated the field intensity factors of a penny-shaped crack in a piezoelectric medium of finite thickness. Li and Lee (2004) investigated the effects of electrical loads on crack growth of penny-shaped dielectric cracks in a piezoelectric layer.

On the other hand, piezoelectric materials are often subjected to dynamic loads in practical applications. It is, therefore, of great importance to investigate the dynamic response of cracked piezoelectric materials, and great progress in this area has been made as well. For example, Dascalu and Maugin (1995) investigated the dynamic fracture of piezoelectric materials by the quasielectrostatic approximation. Li and Mataga (1996a, 1996b) studied a pair of concentrated longitudinal shear loads that suddenly act on the crack surfaces and move at a constant velocity along the crack surfaces far away from the crack tips, and derived the dependence of the field intensity factors and the ERR on the moving velocity for an electrode crack and a vacuum crack, respectively. Chen and Karihaloo (1999) and Chen and Yu (1999) investigated an impermeable finite crack situated in a piezoelectric medium and two coplanar cracks situated in a piezoelectric strip subjected to impact loads, where numerical stress intensity factors have been determined by the numerical solution of a Fredholm integral equation. Wang and Yu (2000) studied the mode-III problem of a crack in piezoelectric strip subjected to the mechanical and electrical impacts by solving numerically resulting Cauchy integral equations. Wang *et al.* (2000) investigated the multiple impermeable crack problems for multilayered piezoelectric materials. Kwon and Lee (2000) analyzed the transient response of a rectangular piezoelectric body with a center crack. Li (2001) and Li and Fan (2002) investigated the transient response of a piezoelectric material with a semi-infinite impermeable mode-III crack under impact loads and the problem of a through permeable crack situated in the mid-plane of a piezoelectric strip under anti-plane impact loads, respectively. Feng *et al.* (2004) studied the transient response of multiple electric permeable coplanar interface cracks between dissimilar piezoelectric materials. Ing and Wang (2004) investigated the transient response of a semi-infinite propagating crack subjected to dynamic anti-plane concentrated loading in a piezoelectric medium. Wang and Yu (2001) studied the transient response of mode-I crack in a piezoelectric strip under the in-plane mechanical and electrical impacts. Gu *et al.* (2002a, 2002b) respectively investigated the mode-I problems of an interface crack between two dissimilar piezoelectric layers for electrically impermeable and electrically permeable crack surface conditions. Chen *et al.* (2003) analyzed the mode-I problem of a crack in a functionally graded piezoelectric medium. However, to the best of our knowledge, to date, the analysis on dynamic behaviors of a penny-shaped crack in a piezoelectric material has not been reported.

In this paper, the problem of a penny-shaped crack in a piezoelectric layer of finite thickness under electromechanical impacts is investigated. Both structure and loads applied are axisymmetrical.

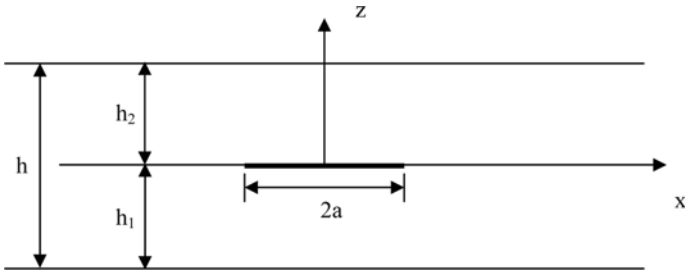

Fig. 1 A penny-shaped crack in a piezoelectric layer

Two kinds of crack surface conditions are considered. Using integral transform technique, the problem considered is reduced to a Fredholm integral equation of the second kind in the Laplace transform domain. The Laplace inversion is carried out to obtain the dynamic stress intensity factor (DSIF) and dynamic energy release rate (DERR). Numerical results are plotted and discussed finally.

2. Description of the problem

As shown in Fig. 1, a penny-shaped crack with radius a is situated in a piezoelectric layer, the thickness of which is h. The layer contains two parts, the thicknesses of which are h_1 and h_2, respectively. The piezoelectric material is transversely isotropic and polarized along the z-axis perpendicular to the crack plane. Assume that the boundaries of piezoelectric layer are subjected to mechanical and electric impacts simultaneously and both the mechanical loadings and electrical loadings are axisymmetrical. For this case, all the field variables are the functions of r and z only.

The governing equations for displacements and electric potential of the present problem are

$$c_{11}\left(\frac{\partial^2 u_{(i)}}{\partial r^2}+\frac{1}{r}\frac{\partial u_{(i)}}{\partial r}-\frac{u_{(i)}}{r^2}\right)+c_{44}\frac{\partial^2 u_{(i)}}{\partial z^2}+(c_{13}+c_{44})\frac{\partial^2 w_{(i)}}{\partial r\,\partial z}+(e_{31}+e_{15})\frac{\partial^2 \phi_{(i)}}{\partial r\,\partial z}=\rho\frac{\partial^2 u_{(i)}}{\partial t^2} \tag{1a}$$

$$c_{44}\left(\frac{\partial^2 w_{(i)}}{\partial r^2}+\frac{1}{r}\frac{\partial w_{(i)}}{\partial r}\right)+c_{33}\frac{\partial^2 w_{(i)}}{\partial z^2}+(c_{13}+c_{44})\left(\frac{\partial^2 u_{(i)}}{\partial r\,\partial z}+\frac{1}{r}\frac{\partial u_{(i)}}{\partial z}\right)+e_{15}\left(\frac{\partial^2 \phi_{(i)}}{\partial r^2}+\frac{1}{r}\frac{\partial \phi_{(i)}}{\partial r}\right)$$
$$+e_{33}\frac{\partial^2 \phi_{(i)}}{\partial z^2}=\rho\frac{\partial^2 w_{(i)}}{\partial t^2} \tag{1b}$$

$$(e_{31}+e_{15})\left(\frac{\partial^2 u_{(i)}}{\partial r\,\partial z}+\frac{1}{r}\frac{\partial u_{(i)}}{\partial z}\right)+e_{15}\left(\frac{\partial^2 w_{(i)}}{\partial r^2}+\frac{1}{r}\frac{\partial w_{(i)}}{\partial r}\right)+e_{33}\frac{\partial^2 w_{(i)}}{\partial z^2}-\varepsilon_{11}\left(\frac{\partial^2 \phi_{(i)}}{\partial r^2}+\frac{1}{r}\frac{\partial \phi_{(i)}}{\partial r}\right)$$
$$-\varepsilon_{33}\frac{\partial^2 \phi_{(i)}}{\partial z^2}=0 \tag{1c}$$

where $u_{(i)}(r,z,t)$ and $w_{(i)}(r,z,t)$ are displacements in r and z directions, respectively; $\phi_{(i)}(r,z,t)$ is the electric potential; c_{ij}, e_{ij}, ε_{ii}, and ρ are elastic constant, piezoelectric constant, dielectric

permittivity, and mass density, respectively. Subscripts $i=1$ and $i=2$ are attached to the lower and upper parts of the piezoelectric layer, respectively.

Constitutive equations are

$$\begin{Bmatrix} \sigma_{rr(i)} \\ \sigma_{\theta\theta(i)} \\ \sigma_{zz(i)} \\ \sigma_{rz(i)} \end{Bmatrix} = \begin{bmatrix} c_{11} & c_{12} & c_{13} & 0 \\ c_{12} & c_{11} & c_{13} & 0 \\ c_{13} & c_{13} & c_{33} & 0 \\ 0 & 0 & 0 & c_{44} \end{bmatrix} \begin{Bmatrix} \partial u_{(i)}/\partial r \\ u_{(i)}/r \\ \partial w_{(i)}/\partial z \\ \partial u_{(i)}/\partial z + \partial w_{(i)}/\partial r \end{Bmatrix} + \begin{bmatrix} 0 & e_{31} \\ 0 & e_{31} \\ 0 & e_{33} \\ e_{15} & 0 \end{bmatrix} \begin{Bmatrix} \partial \phi_{(i)}/\partial r \\ \partial \phi_{(i)}/\partial z \end{Bmatrix} \tag{2a}$$

$$\begin{cases} D_{r(i)} = e_{15}(\partial u_{(i)}/\partial z + \partial w_{(i)}/\partial r) - \varepsilon_{11}\partial \phi_{(i)}/\partial r \\ D_{z(i)} = e_{31}(\partial u_{(i)}/\partial r + u_{(i)}/r) + e_{33}\partial w_{(i)}/\partial z - \varepsilon_{33}\partial \phi_{(i)}/\partial z \end{cases} \tag{2b}$$

where $\sigma_{ij}(r,z,t)$ and $D_i(r,z,t)$ are stress and electric displacement, respectively.

For electrically impermeable crack, the boundary conditions and interface continuity conditions are

$$\{T_1(r, z=-h_1, t)\} = \{t_1(r,t)\} \tag{3a}$$

$$\{T_2(r, z=h_2, t)\} = \{t_2(r,t)\} \tag{3b}$$

$$\{T_1(r, z=0, t)\} = \{T_2(r, z=0, t)\}; \quad r>a \tag{3c}$$

$$\{V_1(r, z=0, t)\} = \{V_2(r, z=0, t)\}; \quad r>a \tag{3d}$$

$$\{T_1(r, z=0, t)\} = \{T_2(r, z=0, t)\} = \{0 \;\; 0 \;\; 0\}^T; \quad r<a \tag{3e}$$

For electrically permeable crack, the boundary conditions and interface continuity conditions are

$$\{T_1(r, z=-h_1, t)\} = \{t_1(r,t)\} \tag{4a}$$

$$\{T_2(r, z=h_2, t)\} = \{t_2(r,t)\} \tag{4b}$$

$$\{T_1(r, z=0, t)\} = \{T_2(r, z=0, t)\}; \quad r>a \tag{4c}$$

$$\{V_1(r, z=0, t)\} = \{V_2(r, z=0, t)\}; \quad r>a \tag{4d}$$

$$\{T_1(r, z=0, t)\} = \{T_2(r, z=0, t)\} = \{0 \;\; 0 \;\; D_{z0}(r,t)\}^T; \quad r<a \tag{4e}$$

where

$$\{T_i(r,z,t)\} = \{\sigma_{zr(i)}(r,z,t)\sigma_{zz(i)}(r,z,t)D_{z(i)}(r,z,t)\}^T \tag{5a}$$

$$\{V_i(r,z,t)\} = \{u_{(i)}(r,z,t)w_{(i)}(r,z,t)\phi_{(i)}(r,z,t)\}^T \tag{5b}$$

$$\{t_i(r,t)\} = \{\tau_i(r,t)\sigma_i(r,t)D_i(r,t)\}^T \tag{5c}$$

and $\tau_i(r,t)$, $\sigma_i(r,t)$ and $D_i(r,t)$ are the known loads applied on the surfaces of the piezoelectric layer, respectively. $D_{z0}(r,t)$ is an unknown function to be determined.

3. Solution of the problem

We proceed with the electrically impermeable case. Introducing the Laplace transform and defining

$$f^*(p) = \int_0^\infty f(t)e^{-pt}dt \tag{6}$$

Eq. (1) can be converted into

$$c_{11}\left(\frac{\partial^2 u^*_{(i)}}{\partial r^2}+\frac{1}{r}\frac{\partial u^*_{(i)}}{\partial r}-\frac{u^*_{(i)}}{r^2}\right)+c_{44}\frac{\partial^2 u^*_{(i)}}{\partial z^2}+(c_{13}+c_{44})\frac{\partial^2 w^*_{(i)}}{\partial r\,\partial z}+(e_{31}+e_{15})\frac{\partial^2 \phi^*_{(i)}}{\partial r\,\partial z}=\rho p^2 u^*_{(i)} \tag{7a}$$

$$c_{44}\left(\frac{\partial^2 w^*_{(i)}}{\partial r^2}+\frac{1}{r}\frac{\partial w^*_{(i)}}{\partial r}\right)+c_{33}\frac{\partial^2 w^*_{(i)}}{\partial z^2}+(c_{13}+c_{44})\left(\frac{\partial^2 u^*_{(i)}}{\partial r\,\partial z}+\frac{1}{r}\frac{\partial u^*_{(i)}}{\partial z}\right)+e_{15}\left(\frac{\partial^2 \phi^*_{(i)}}{\partial r^2}+\frac{1}{r}\frac{\partial \phi^*_{(i)}}{\partial r}\right)$$
$$+e_{33}\frac{\partial^2 \phi^*_{(i)}}{\partial z^2}=\rho p^2 w^*_{(i)} \tag{7b}$$

$$(e_{31}+e_{15})\left(\frac{\partial^2 u^*_{(i)}}{\partial r\,\partial z}+\frac{1}{r}\frac{\partial u^*_{(i)}}{\partial z}\right)+e_{15}\left(\frac{\partial^2 w^*_{(i)}}{\partial r^2}+\frac{1}{r}\frac{\partial w^*_{(i)}}{\partial r}\right)+e_{33}\frac{\partial^2 w^*_{(i)}}{\partial z^2}-\varepsilon_{11}\left(\frac{\partial^2 \phi^*_{(i)}}{\partial r^2}+\frac{1}{r}\frac{\partial \phi^*_{(i)}}{\partial r}\right)$$
$$-\varepsilon_{33}\frac{\partial^2 \phi^*_{(i)}}{\partial z^2}=0 \tag{7c}$$

The solution to Eq. (7) is of the form

$$\{V_i^*(r,z,p)\} = \int_0^\infty F_{(i)}(s)\{A_{1(i)}(s,p)J_1(sr)\;\; A_{3(i)}(s,p)J_0(sr)\;\; A_{4(i)}(s,p)J_0(sr)\}^T e^{s\lambda_{(i)}(s,p)z}ds \tag{8}$$

where $F_{(i)}(s)$ is an unknown function to be determined, $\lambda_{(i)}(s,p)$ and $\{A_{1(i)}(s,p)\;\; A_{3(i)}(s,p)\;\; A_{4(i)}(s,p)\}^T$ are, respectively, eigenvalue and eigenvector of the following characteristic equation

$$\begin{bmatrix} c_{11}-c_{44}\lambda^2_{(i)}+\dfrac{\rho p^2}{s^2} & (c_{13}+c_{44})\lambda_{(i)} & (e_{31}+e_{15})\lambda_{(i)} \\ (c_{13}+c_{44})\lambda_{(i)} & c_{33}\lambda^2_{(i)}-c_{44}-\dfrac{\rho p^2}{s^2} & e_{33}\lambda^2_{(i)}-e_{15} \\ (e_{31}+e_{15})\lambda_{(i)} & e_{33}\lambda^2_{(i)}-e_{15} & \varepsilon_{11}-\varepsilon_{33}\lambda^2_{(i)} \end{bmatrix}\begin{Bmatrix} A_{1(i)} \\ A_{3(i)} \\ A_{4(i)} \end{Bmatrix} = \begin{Bmatrix} 0 \\ 0 \\ 0 \end{Bmatrix} \tag{9}$$

Six roots for $\lambda_{(i)}$ in Eq. (9) can been found, which are expressed as $\lambda_{\alpha(i)}(\alpha = 1, 2, \ldots, 6)$. In terms of these eigenvalues and eigenvectors, a general expression for the displacements and electric potential can be rewritten as

$$\{V_i^*(r,z,p)\} = \int_0^\infty [G(sr)][A^{(i)}(s,z,p)]\{F_{(i)}(s)\}ds \tag{10}$$

where

$$[G(sr)] = diag[J_1(sr), J_0(sr), J_0(sr)] \tag{11}$$

$$[A^{(i)}(s,z,p)] = \begin{bmatrix} A_{11(i)}(s,p)e^{s\lambda_{1(i)}(s,p)z} & A_{12(i)}(s,p)e^{s\lambda_{2(i)}(s,p)z} & \ldots & A_{16(i)}(s,p)e^{s\lambda_{6(i)}(s,p)z} \\ A_{31(i)}(s,p)e^{s\lambda_{1(i)}(s,p)z} & A_{32(i)}(s,p)e^{s\lambda_{2(i)}(s,p)z} & \ldots & A_{36(i)}(s,p)e^{s\lambda_{6(i)}(s,p)z} \\ A_{41(i)}(s,p)e^{s\lambda_{1(i)}(s,p)z} & A_{42(i)}(s,p)e^{s\lambda_{2(i)}(s,p)z} & \ldots & A_{46(i)}(s,p)e^{s\lambda_{6(i)}(s,p)z} \end{bmatrix} \tag{12}$$

$$\{F_{(i)}(s)\} = \{F_{1(i)}(s) \;\; F_{2(i)}(s) \;\; \ldots \;\; F_{6(i)}(s)\}^T \tag{13}$$

Making use of Eq. (2), the stresses and electric displacement are obtained as

$$\{T_i^*(r,z,p)\} = \int_0^\infty s[G(sr)][B^{(i)}(s,z,p)]\{F_{(i)}(s)\}ds \tag{14}$$

where $B^{(i)}(r,z,p)$ is a matrix of 3×6, the elements of which are

$$B_{1\alpha}^{(i)}(s,z,p) = (c_{44}\lambda_{\alpha(i)}(s,p)A_{1\alpha(i)}(s,p) - c_{44}\lambda_{3\alpha(i)}(s,p) - e_{15}A_{4\alpha(i)}(s,p))e^{s\lambda_{\alpha(i)}(s,p)z} \tag{15a}$$

$$B_{2\alpha}^{(i)}(s,z,p) = (c_{13}A_{1\alpha(i)}(s,p) + c_{33}\lambda_{\alpha(i)}(s,p)A_{3\alpha(i)}(s,p) + e_{33}\lambda_{\alpha(i)}(s,p)A_{4\alpha(i)}(s,p))e^{s\lambda_{\alpha(i)}(s,p)z} \tag{15b}$$

$$B_{3\alpha}^{(i)}(s,z,p) = (e_{31}A_{1\alpha(i)}(s,p) + e_{33}\lambda_{\alpha(i)}(s,p)A_{3\alpha(i)}(s,p) - \varepsilon_{33}\lambda_{\alpha(i)}(s,p)A_{4\alpha(i)}(s,p))e^{s\lambda_{\alpha(i)}(s,p)z} \tag{15c}$$

in which $\alpha = 1, 2, \ldots, 6$.

In the Laplace domain, the boundary conditions can be rewritten as

$$\{T_1^*(r, z = -h_1, p)\} = \{t_1^*(r,p)\} \tag{16a}$$

$$\{T_2^*(r, z = h_2, p)\} = \{t_2^*(r,p)\} \tag{16b}$$

$$\{T_1^*(r, z = 0, p)\} = \{T_2^*(r, z = 0, p)\}; \quad r > a \tag{16c}$$

$$\{V_1^*(r, z = 0, p)\} = \{V_2^*(r, z = 0, p)\}; \quad r > a \tag{16d}$$

$$\{T_1^*(r, z = 0, p)\} = \{T_2^*(r, z = 0, p)\} = \{0 \;\; 0 \;\; 0\}^T; \quad r < a \tag{16e}$$

Let $\{t_0^*(r,p)\}$ represent $\{T_1^*(r, z = 0, p)\}$ or $\{T_2^*(r, z = 0, p)\}$. Noting Eq. (16c), the unknown vector $\{F_{(i)}(s)\}$ can be expressed in terms of $\{t_1^*(r,p)\}$ and $\{t_0^*(r,p)\}$ by applying inverse

Hankel transform to Eq. (14) (Wang *et al.* 2001). The result is

$$\{F_{(1)}(s)\} = [C_1(s,p)]\begin{Bmatrix}\Gamma_0(s,p)\\ \Gamma_1(s,p)\end{Bmatrix};\quad \{F_{(2)}(s)\} = [C_2(s,p)]\begin{Bmatrix}\Gamma_2(s,p)\\ \Gamma_0(s,p)\end{Bmatrix} \tag{17}$$

where

$$[C_1(s,p)] = \begin{bmatrix}B^{(1)}(s,0,p)\\ B^{(1)}(s,-h_1,p)\end{bmatrix}^{-1};\quad [C_2(s,p)] = \begin{bmatrix}B^{(2)}(s,h_2,p)\\ B^{(2)}(s,0,p)\end{bmatrix}^{-1} \tag{18}$$

$\{\Gamma_0(s,p)\}$ is the Hankel transform of $\{t_0^*(r,p)\}$, and $\{\Gamma_1(s,p)\}$ and $\{\Gamma_2(s,p)\}$ are the Hankel transforms of $\{t_1^*(r,p)\}$ and $\{t_2^*(r,p)\}$, respectively.

Substitute Eq. (17) into Eq. (10), we have

$$\{V_1^*(r,z,p)\} = \int_0^\infty [G(sr)][D_{11}(s,z,p)\ \ D_{21}(s,z,p)]\begin{Bmatrix}\Gamma_0(s,p)\\ \Gamma_1(s,p)\end{Bmatrix}ds \tag{19a}$$

$$\{V_2^*(r,z,p)\} = \int_0^\infty [G(sr)][D_{12}(s,z,p)\ \ D_{22}(s,z,p)]\begin{Bmatrix}\Gamma_2(s,p)\\ \Gamma_0(s,p)\end{Bmatrix}ds \tag{19b}$$

where

$$[D_{11}(s,z,p)\ \ D_{21}(s,z,p)] = [A^{(1)}(s,z,p)][C_1(s,p)] \tag{20a}$$

$$[D_{12}(s,z,p)\ \ D_{22}(s,z,p)] = [A^{(2)}(s,z,p)][C_2(s,p)] \tag{20b}$$

With the aid of interface continuity condition, i.e., Eq. (16d), we get

$$\int_0^\infty [G(sr)]([L(s,p)]\{\Gamma_1(s,p)\} + [M(s,p)]\{\Gamma_0(s,p)\} + [N(s,p)]\{\Gamma_2(s,p)\})ds = \{0\ \ 0\ \ 0\}^T$$
$$r < a \tag{21}$$

where

$$[L(s,p)] = [D_{21}(s,0,p)] \tag{22a}$$

$$[M(s,p)] = [D_{11}(s,0,p) - D_{22}(s,0,p)] \tag{22b}$$

$$[N(s,p)] = -[D_{12}(s,0,p)] \tag{22c}$$

From Eq. (21), the solution of $\{\Gamma_0(s,p)\}$ can be expressed in terms of an unknown vector $\{d(r,p)\} = \{d_u(r,p)\ \ d_w(r,p)\ \ d_\phi(r,p)\}^T$, $r < a$ as

$$[M(s,p)]\{\Gamma_0(s,p)\} = -[L(s,p)]\{\Gamma_1(s,p)\} - [N(s,p)]\{\Gamma_2(s,p)\} +$$
$$s^{1/2}\int_0^a [\Xi(sr)]\{d(r,p)\}dr \tag{23}$$

where

$$[\Xi(sr)] = diag[J_{3/2}(sr), J_{1/2}(sr), J_{1/2}(sr)] \tag{24}$$

The singularity of crack tip fields is duo to the asymptotic behavior of $[M(s,p)]$ as s tends to infinity. By introducing

$$[K(s,p)] = [M(s,p)]^{-1} - [M(\infty,p)]^{-1} = [M(s,p)]^{-1} - [\Delta]$$

we can obtain from Eq. (23)

$$\{\Gamma_0(s,p)\} = -\{\Gamma_b(s,p)\} + [\Delta]s^{1/2}\int_0^a [\Xi(sx)]\{d(x,p)\}dx + [K(s,p)]s^{1/2}\int_0^a [\Xi(sx)]\{d(x,p)\}dx \tag{25}$$

where

$$\{\Gamma_b(s,p)\} = [M(s,p)]^{-1}[L(s,p)]\{\Gamma_1(s,p)\} + [M(s,p)]^{-1}[N(s,p)]\{\Gamma_2(s,p)\} \tag{26}$$

So far, $\{d(r,p)\}$ in Eq. (25) is the only unknown vector in the present problem, which may be determined from the crack surface condition Eq. (16e):

$$[\Lambda]\int_0^\infty s^{3/2}[G(sr)]\int_0^a [\Xi(sx)]\{d(x,p)\}dxds$$
$$+\int_0^\infty s^{3/2}[G(sr)][K(s,p)]\int_0^a [\Xi(sx)]\{d(x,p)\}dxds = \{\sigma_b^*(r,p)\}; \quad r<a \tag{27}$$

where

$$\{\sigma_b^*(r,p)\} = \int_0^\infty s[G(sr)]\{\Gamma_b(s,p)\}ds \tag{28}$$

Integral Eq. (27) can be further simplified to

$$[\Delta]\{d(r,p)\} + \int_0^\infty [R(r,x,p)]\{d(x,p)\}dx =$$
$$\sqrt{\frac{2}{\pi}}\,diag[1/\sqrt{r}, \sqrt{r}, \sqrt{r}]\int_0^r \frac{1}{\sqrt{r^2-x^2}}diag[x^2, x, x]\{\sigma_b^*(x,p)\}dx \tag{29}$$

The kernel $[R(r,x,p)]$ takes the form

$$[R(r,x,p)] = r\int_0^\infty s\Xi(sr)[K(s,p)]\Xi(sx)ds \tag{30}$$

The numerical solution of Eq. (29) has been obtained using a collocation technique where the function $\{d(r,p)\}$ is found at discrete points by matching the discrete values of the integral equation's non-homogeneous term. Once $\{d(r,p)\}$ is solved from Eq. (29), the DSIF and dynamic electric displacement intensity factor (DEDIF) in the Laplace domain can be obtained as follows

$$\{K^*(p)\} = \{K_{II}^*(p) \;\; K_I^*(p) \;\; K_{IV}^*(p)\}^T = \sqrt{2(r-a)}\{t_0^*(r,p)\}_{r\to a^+} = -\sqrt{\frac{2a}{\pi}}[\Delta]\{d(a,p)\} \tag{31}$$

where mode IV refers to in-plane electric displacement.

From the Laplace inversion

$$f(t) = \frac{1}{2\pi i}\int_{Br} f^*(p)e^{pt}\,dp \tag{32}$$

where Br denotes the Bromwich path of integration, the DSIF and DEDIF in the time domain can be obtained as

$$\{K(t)\} = -\sqrt{\frac{2a}{\pi}}[\Delta]\frac{1}{2\pi i}\int_{Br}\{d(a,p)\}e^{pt}\,dp \tag{33}$$

The Laplace inversion in Eq. (33) can be carried out by the numerical method given by Miller and Guy (1966).

As well known, for electrically impermeable cracks, the DERR as a fracture parameter is more appropriate than the DSIF. For the present problem, the DERR $G(t)$ can be finally evaluated by the crack closure integral technique. The result is

$$G(t) = \frac{1}{a\sqrt{a}}\{K(t)\}^T[\Delta]^{-1}\{K(t)\} \tag{34}$$

For electrically permeable case, the singular integral equation can be derived by a similar method as

$$[\Omega]\int_0^\infty s^{3/2}[E(sr)]\int_0^a[\Sigma(sx)]g(x,p)dxds$$
$$+\int_0^\infty s^{3/2}[E(sr)][\Phi(s,p)]\int_0^a[\Sigma(sx)]g(x,p)dxds = \{\varsigma_b^*(r,p)\};\quad r<a \tag{35}$$

where

$$\Omega_{ij} = \Delta_{ij};\quad i,j = 1,2 \tag{36a}$$

$$\Phi_{ij} = K_{ij};\quad i,j = 1,2 \tag{36b}$$

$$[E(sr)] = diag[J_1(sr), J_0(sr)] \tag{36c}$$

$$[\Sigma(sr)] = diag[J_{3/2}(sr), J_{1/2}(sr)] \tag{36d}$$

$$\{g(r,p)\} = \{d_u(r,p)\quad d_w(r,p)\}^T \tag{36e}$$

$$\varsigma_{b_i} = \sigma_{b_i},\quad i = 1,2 \tag{36f}$$

And D_{z0} can be obtained as

$$D_{z0}^*(r,p) = \int_0^\infty\int_0^a s^{3/2}(\Delta_{31}d_u(r,p)J_1(sr)J_{3/2}(sx) + \Delta_{32}d_w(r,p)J_0(sr)J_{1/2}(sx))dsdx +$$
$$\int_0^\infty\int_0^a s^{3/2}(K_{31}d_u(r,p)J_1(sr)J_{3/2}(sx) + K_{32}d_w(r,p)J_0(sr)J_{1/2}(sx))dsdx \tag{37}$$

The DSIF and DERR in the time domain can be finally obtained as

$$\{K(t)\} = -\sqrt{\frac{2a}{\pi}}[\Omega]\frac{1}{2\pi i}\int_{Br}\{g(a,p)\}e^{pt}dp \tag{38}$$

$$G(t) = \frac{1}{a\sqrt{a}}\{K_{II}(t)\ \ K_I(t)\}^T[\Omega]^{-1}\{K_{II}(t)\ \ K_I(t)\} \tag{39}$$

Eqs. (38) and (39) show that both the DSIF and DERR are independent of electrical loadings. Eq. (39) also implies that the DERR as a fracture parameter is equivalent to the DSIF in the view of fracture mechanics for electrically permeable cracks.

4. Numerical example and discussion

In this section, the fracture properties of piezoelectric ceramics with cracks are investigated. The piezoelectric material is taken as PZT-5H, the material constants of which are respectively $c_{11} = 12.6 \times 10^{10}$ N/m^2, $c_{13} = 5.3 \times 10^{10}$ N/m^2, $c_{33} = 11.7 \times 10^{10}$ N/m^2, $c_{44} = 3.53 \times 10^{10}$ N/m^2, $e_{31} = -6.5$ C/m^2, $e_{33} = 23.3$ C/m^2, $e_{15} = 17.0$ C/m^2, $\varepsilon_{11} = 151 \times 10^{-10}$C/Vm, $\varepsilon_{33} = 130 \times 10^{-10}$ C/Vm, $\rho = 7500$ kg/m^3. Firstly calculated are the DERR and DSIF for electrically impermeable cracks. For simplicity, we directly set $\{t_1(r,t)\} = \{t_2(r,t)\} = \{0\ \ \sigma_0 H(t)\ \ D_0 H(t)\}^T$, where $H(t)$ is the Heaviside unit step function. In all our numerical procedure σ_0 is taken as 4.2×10^6 N/m^2, and D_0 is determined by the load combination parameter λ, which is defined as $\lambda = D_0 c_{33}/(\sigma_0 e_{33})$.

Numerical results are plotted in Figs. 2-5, where the DERR is normalized by G_0, i.e., the static ERR for infinite piezoelectric material without electric displacement loadings, the DSIF is normalized by $\sigma_0 a^{1/2}$, and the normalized time is taken as $(c_{33}/\rho)^{1/2} t/a$. From these figures, it is easy to know that both the DERR and DSIF rise quickly to reach the peak values, then drop slowly, and finally approach to the corresponding static values, and that the peak values appear at $(c_{33}/\rho)^{1/2} t/a = 0.5 \sim 1.0$. As shown in Figs. 2 and 3, both the DERR and DSIF tend to decrease with the increasing of h/a. The peak values of the DERR are higher than the corresponding static

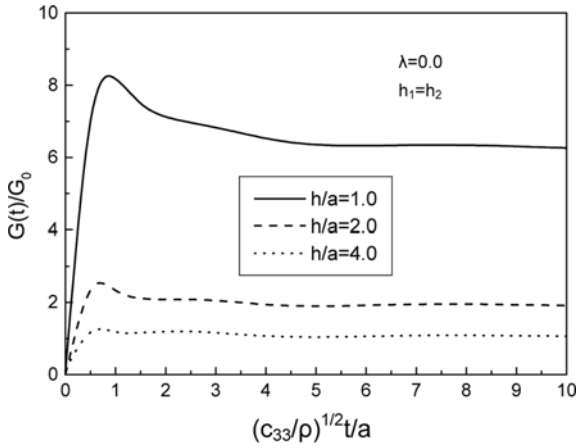

Fig. 2 Normalized DERR versus normalized time for different values of h/a for electrically impermeable crack

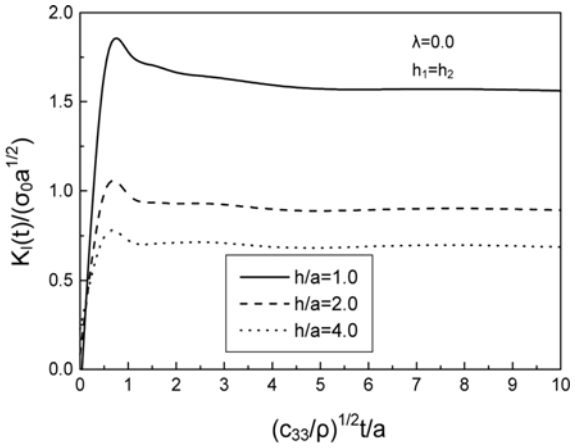

Fig. 3 Normalized DSIF versus normalized time for different values of h/a for electrically impermeable crack

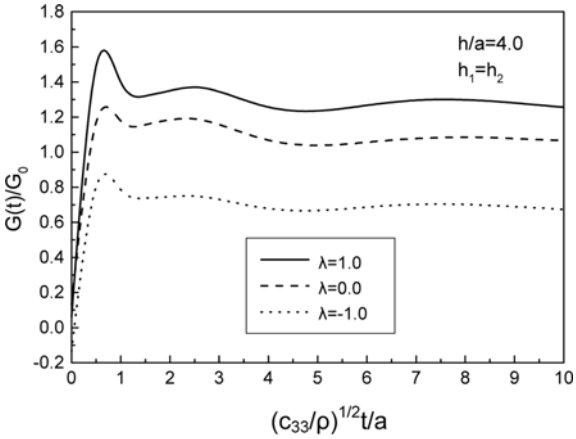

Fig. 4 Normalized DERR versus normalized time for different values of λ for electrically impermeable crack

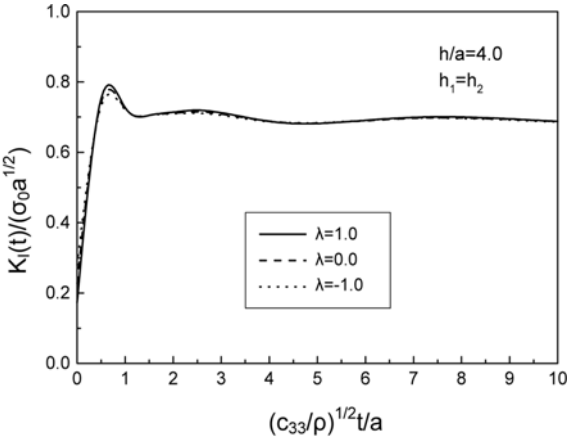

Fig. 5 Normalized DSIF versus normalized time for different values of λ for electrically impermeable crack

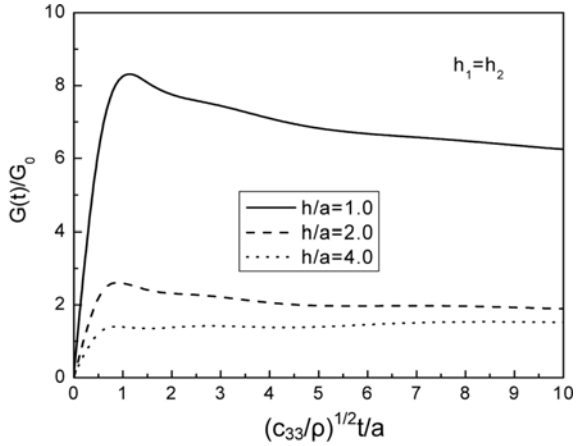

Fig. 6 Normalized DERR versus normalized time for different values of *h/a* for electrically permeable crack

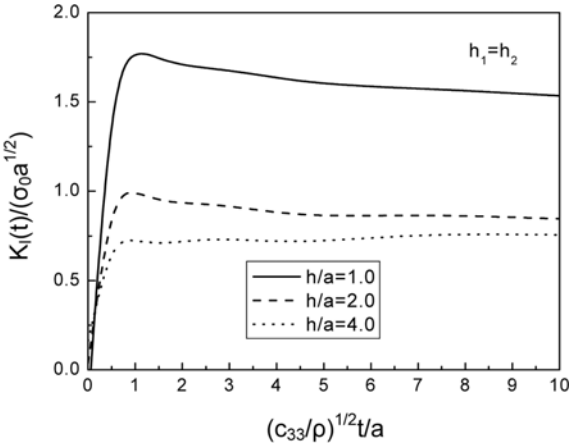

Fig. 7 Normalized DSIF versus normalized time for different values of *h/a* for electrically permeable crack

values by about 30%, 20%, and 10% for $h/a = 1.0$, $h/a = 2.0$, and $h/a = 4.0$, respectively. However, for different ratios of the thickness of the layer to the length of the crack, the peak values of the DSIF are higher than the corresponding static values by about 10%. Fig. 4 indicates that for electrically impermeable cracks, positive electric displacement loadings can increase the DERR, while negative electric displacement loadings can decrease the DERR. This means that the negative electric displacement loadings can be properly applied to inhibit crack growth. Fig. 5 implies that the DSIF is independent of electric displacement loadings. In fact, this phenomenon has been observed for static case.

Finally, the DERR and DSIF for electrically permeable cracks are evaluated. Noting that electric displacement loadings have no effects on the fracture behaviors of the crack, we directly set $\{t_1(r,t)\} = \{t_2(r,t)\} = \{0 \;\; \sigma_0 H(t) \;\; 0\}^T$. Numerical results are plotted in Figs. 6 and 7. Comparing

Fig. 6 with Fig. 2 and/or Fig. 7 with Fig. 3, we can see that the results of electrically permeable cracks haven't obvious differences with the corresponding results of the electrically impermeable cracks under only mechanical loadings.

5. Conclusions

In this paper, a penny-shaped crack in a piezoelectric layer under electromechanical impacts is investigated. Two kinds of crack surface conditions are adopted. From the numerical results, the following conclusions can be drawn.

(1) In the loading process, the peak values of the DSIF or DERR usually occur at $(c_{33}/\rho)^{1/2}t/a = 0.5\sim1.0$.
(2) With the decreasing of h/a, the dynamic loadings have more significant influences on the peak value of the DERR.
(3) For electrically impermeable cracks, electric displacement loadings have no influences on the DSIF. However, they have obvious influences on the DERR. And positive electric displacement loadings can enhance crack propagation and growth, while negative electric displacement loadings can inhibit crack growth.
(4) For electrically permeable cracks, electric displacement loadings have no influences on the DERR and DSIF.

References

Chen, J., Liu, Z.X. and Zou, Z.Z. (2003), "Electromechanical impact of a crack in a functionally graded piezoelectric medium", *Theor. Appl. Fract. Mech.*, **39**, 47-60.
Chen, W.Q. and Shioya, T. (1999), "Fundamental solution for a penny-shaped crack in a piezoelectric medium", *J. Mech. Phys. Solids*, **47**, 1459-1475.
Chen, W.Q. and Shioya, T. (2000), "Complete and exact solutions of a penny-shaped crack in a piezoelectric solid: Antisymmetric shear loadings", *Int. J. Solids Struct.*, **37**, 2603-2619.
Chen, W.Q., Shioya, T. and Ding, H.J. (2000), "Penny-shaped crack in piezoelectrics: Resolved", *Int. J. Fract.,* **105**, 49-56.
Chen, Z.T. and Karihaloo, B.H. (1999), "Dynamic response of a cracked piezoelectric ceramic under arbitrary electro-mechanical impact", *Int. J. Solids Struct.*, **36**, 5125-5133.
Chen, Z.T. and Yu, S.W. (1999), "Transient response of a piezoelectric ceramic with two coplanar cracks under electromechanical impact", *Acta Mech. Sinica*, **15**, 325-333.
Dascalu, C. and Maugin, G. (1995), "On the dynamic fracture of piezoelectric materials", *Q. J. Mech. Appl. Math.*, **48**, 237-255.
Deeg, W.F. (1980), "The analysis of dislocation, crack, and inclusion problems in piezoelectric solids", Ph.D. Thesis, Stanford University, USA.
Eriksson, K. (2002), "Energy release rates for the penny-shaped crack in a linear piezoelectric solid", *Int. J. Fract.,* **116**, L23-L28.
Feng, W.J., Su, R.K.L. and Zou, Z.Z. (2004), "Dynamic response of multiple coplanar interface cracks between two dissimilar piezoelectric materials", *Key Engn. Mater.*, **261-263**, 477-482.
Gu, B., Yu, S.W. and Feng, X.Q. (2002a), "Transient response of an insulating crack between piezoelectric layers under mechanical and electrical impacts", *Arch. Appl. Mech.,* **72**, 615-629.
Gu, B., Yu, S.W. and Feng, X.Q. (2002b), "Transient response of an interface crack between piezoelectric layers under mechanical impacts", *Int. J. Solids Struct.*, **39**, 1743-1756.

Ing, Y.S. and Wang, M.J. (2004), "Transient analysis of a mode-III crack propagating in a piezoelectric medium", *Int. J. Solids Struct.*, **41**, 6197-6214.
Karapetian, E., Sevotianov, I. and Kachanov, M. (2000), "Penny-shaped and half-plane cracks in a transversely isotropic piezoelectric solid under arbitrary loading", *Arch. Appl. Mech.,* **70**, 201-229.
Kogan, L., Hui, C.Y. and Molkov, V. (1996), "Stress and induction field of a spherical inclusion or a penny-shaped crack in a transversely isotropic piezoelectric material", *Int. J. Solids Struct.,* **33**, 2719-2737.
Kwon, S.M. and Lee, K.Y. (2000), "Transient response of a rectangular medium with a center crack", *Eur. J. Mech. A/Solids*, **20**, 457-468.
Li, S.F. and Mataga, P.A. (1996a), "Dynamic crack propagation in piezoelectric materials – Part 1: Electrode solution", *J. Mech. Phys. Solids,* **44**, 1799-1830.
Li, S.F. and Mataga, P.A. (1996b), "Dynamic crack propagation in piezoelectric materials – Part 2: Vacuum solution", *J. Mech. Phys. Solids,* **44**, 1831-1866.
Li, X.F. (2001), "Transient response of a piezoelectric material with a semi-infinite mode-III crack under impact loads", *Int. J. Fract.*, **111**, 119-130.
Li, X.F. and Fan, T.Y. (2002), "Transient analysis of a piezoelectric strip with a permeable crack under anti-plane impact loads", *Int. J. Eng. Sci.,* **40**, 131-143.
Li, X.F. and Lee, K.Y. (2004), "Effects of electric field on crack growth for a penny-shaped dielectric crack in a piezoelectric layer", *J. Mech. Phys. Solids.,* **52**, 2079-2100.
Lin, S., Narita, F. and Shindo, Y. (2003), "Electroelastic analysis of a penny-shaped crack in a piezoelectric ceramic under mode-I loading", *Mech. Res. Commu.,* **30**, 371-386.
Miller, M.K. and Guy, W.T. (1966), "Numerical inversion of the Laplace transform by use of Jacobi polynomials", *SIAM J. Numer. Anal.,* **3**, 624-635.
Parton, V.Z. (1976), "Fracture mechanics of piezoelectric materials", *Acta Astro.,* **3**, 671-683.
Wang, B.L., Han, J.C. and Du, S.Y. (2000), "Electroelastic fracture dynamics for multilayered piezoelectric materials under dynamic anti-plane shearing", *Int. J. Solids Struct.*, **37**, 5219-5231.
Wang, B.L., Noda, N., Han, J.C. and Du, S.Y. (2001), "A penny-shaped crack in a transversely isotropic piezoelectric layer", *Eur. J. Mech. A/Solids,* **20**, 997-1005.
Wang, X.Y. and Yu, S.W. (2000), "Transient response of a crack in piezoelectric strip subjected to mechanical and impacts: mode-III problem", *Int. J. Solids Struct.*, **37**, 5795-5808.
Wang, X.Y. and Yu, S.W. (2001), "Transient response of a crack in piezoelectric strip subjected to mechanical and impacts: mode-I problem", *Mech. Mater.,* **33**, 11-20.
Yang, F.Q. (2004), "General solutions of a penny-shaped crack in a piezoelectric material under opening mode-I loading", *Quart. J. Mech. Appl. Math.,* **57**, 529-550.
Yang, J.H. and Lee, K.Y. (2003a), "Penny-shaped crack in a piezoelectric cylinder under electromechanical loads", *Arch. Appl. Mech.,* **73**, 323-336.
Yang, J.H. and Lee, K.Y. (2003b), "Penny-shaped crack in a piezoelectric cylinder surrounded by an elastic medium subjected to combined in-plane mechanical and electrical loads", *Int. J. Solids Struct.,* **40**, 573-590.